Lyman-α ~~emission reveals~~ Line Sketches a ~~dispersion-supported dwarf~~Massive Dwarf Galaxy

Jaime E. Forero-Romero[1], Max Groenke[2], María Camila Remolina-Gutiérrez[1], Juan Nicolás Garavito-Carmargo[3], Mark Dijkstra[2].

[1] Departamento de Física, Universidad de los Andes, Cra. 1 No. 18A-10 Edificio Ip, CP 111711, Bogotá, Colombia

[2] Institute of Theoretical Astrophysics, University of Oslo, Postboks 1029 Blindern, NO-0315 Oslo, Norway.

[3] Department of Astronomy, University of Arizona, 933 North Cherry Avenue, Tucson, AZ 85721, USA.

Star-forming Compact Dwarf Galaxies (CDGs) resemble the expected pristine conditions of the first galaxies in the Universe. Before the observational detection of the first galaxies becomes reality, CDGs are the best systems to test our ideas on primordial galaxy formation and evolution. Here we report on one of such CDGs, Tololo 1214-277, which presents a broad symmetric Lyman-α line emission that had evaded theoretical interpretation so far. In this letter we explain these features by two different models: an homogeneous gaseous sphere undergoing bulk rotation and an interstellar medium composed by outflowing clumps with additional random motions. It is the first time that an observed Lyα spectrum can be explained assuming either of these physical conditions. We find that both models independently require high velocities (either a bulk rotation of 348^{+75}_{-48} km s^{-1} or a clump velocity dispersion of ~~69^{+17}_{-15} km s^{-1}~~ 54.3 ± 0.6 km s^{-1}with outflows of ~~79^{+73}_{-42} km s^{-1}~~54.3 ± 5.1 km s^{-1}) consistent with a dynamical mass of at least ~~10~~ a billion solar masses, 6 times larger than its baryonic mass. We argue that ~~the most plaussible~~ a possible explanation for this excess of dynamical mass is ~~provided by~~ the ~~multiphase model as it is~~ presence of a ~~close match to~~ supermassive black hole at the ~~galaxy scaling relationship for a dark matter dominated dwarf elliptical supported by its velocity dispersion~~center of Tololo 1214-277. This work demonstrates the importance of considering multiphase physics and rotation among the possible conditions shaping the Lyα spectra of the first galaxies. Additionally, if future kinematic maps of Tololo 1214-277 confirm the high velocities postulated in our model, it would ~~help to stablish the Lyαline morphology~~ provide new evidence for dwarf galaxies as ~~an observational tracer to study the co-evolution of the first generation~~ hosts of ~~galaxies and its host dark matter halos~~supermassive black holes.

The first generation of galaxies trace our cosmic origins. They were the first steps in the evolution of galaxies such as the Milky Way. In the standard Big Bang cosmology the only chemical elements that were created in the nucleosynthesis process were Hydrogen, Helium and Lithium. Heavier elements must have been created in stellar evolution process. Therefore, we expect the first generation of galaxies to be metal free and rich in Hydrogen. This kind of primordial galaxies have not been detected yet. However, dwarf star forming galaxies with a low metallicity content are seen as templates to understand the early galaxy evolution process.

Almost fifty years ago [1] it was realized that young galaxies could be detected through a strong Lyman-α line emission. This theoretical prediction was only confirmed thirty ~~year~~ years later on distant, relatively young, not primordial, galaxies [2] . Currently Lyman Alpha Emitting (LAE) galaxies are commonly targeted in surveys. The presence of the Ly-α emission line provides confirmation of the distance of a galaxy while provides clues about the stellar population and inter-stellar medium conditions regulating the Ly-α emission.

The Ly-α emission line is not exclusive of distant galaxies. Any galaxy with low dust content and ongoing star formation has the right conditions to show this line. There are, for instance, local Universe surveys that target Ly-α emission in nearby dwarf star forming galaxies [3]. The study of nearby LAE samples has allowed the study of other indicators that might be more difficult to obtain for distant galaxies such as morphology, dust attenuation, neutral hydrogen contents and ionization state.

However, the physical interpretation of Ly-α observations is not straightforward [4] . This is due to the resonant nature of the Ly-α line. A Ly-α photon follows a diffusion-like process before escaping the galaxy or being absorbed by dust. The resulting line profile becomes sensitive to the dynamical, chemical and thermal conditions in the interstellar medium. There are very few analytically tools available to interpret the emerging Ly-α line. They are applicable only in very few cases of highly symmetrical conditions, which are hardly met in real astrophysical systems. For these reasons the interpretation of Ly-α observations ~~require~~ requires state-of-the-art Monte Carlo radiative transfer simulations. ~~Recent advances in these computational models have explored the effects that bulk rotation and a multiphase state in the interstellar medium should have on the Lyman-α line.~~

~~The most important consequence of bulk rotation is that, even for a spherical gas distribution, the line morphology now depends on the viewing angle respect to the rotation axis. For a line of sight perpendicular to the rotation axis the intensity and the line center and the line width increase with rotational velocity. When the rotational velocity is high enough, the line becomes single peaked and symmetric, a unique feature that other theoretical models find difficult to reproduce without introducing more complexity into the gas distribution.~~

~~This is the case of a multiphase interstellar medium. The model is more complex as it must take into account the behavior of neutral dense hydrogen clumps dispersed in a tenuous intraclump medium. Corresponding to the elaborate physical conditions in the model, there are a wide variety of possible emerging spectra. This variety includes single, double and triple peaked spectra with different degrees of symmetry around the line's center.~~

Tololo 1214-277 is a compact star forming dwarf galaxy that presents a strong Ly-α emission [5] with two puzzling features: ~~it~~ the line is symmetric and single peaked. ~~Commonly,~~ Usually the Ly-α line has ~~a single or asymmetric~~ an asymmetric single or double peak. These two special features in Tololo 1214-277 ~~had evaded a physical interpretation so far. Including the effects of either bulk rotationor a multiphase ISM, we manage to explain the Lyαline in Tololo 1214-277.~~ cannot be explained with conventional models [6, 7] .

In this letter we show how the Tololo 1214-277's Lyα profile can be explained either by rotation [8] or the recently developed class of more complex multiphase models that predict a wider variety of spectra including, single, double and triply peaked spectra [9] . Figure 1. summarizes our findings. Dots represent the observational data for Tololo 1214-277 with the overplot from our best ~~fit models from the full radiative transfer simulations~~ fits from the analytical solution for a rotating ~~sphere (continuous~~ homogeneous gas sphere (thin line) and ~~a clumpy ISM (dashed~~ the multiphase model (thick line). This is the first time that these models have been introduced with success to explain an observed Lyα profile.

The best parameters in the rotation model are a rotational velocity of $V_{\rm max} = 348^{+75}_{-48}$ km s^{-1}, ~~an optical depth~~ a neutral Hydrogen optical depth of $\log_{10}\tau = 6.96^{+0.26}_{-0.18}$, and ~~a~~ an inter-stellar medium temperature of $\log_{10} T/{\rm K} = 4.27^{+0.11}_{-0.18}$. This model is also able to constrain the angle between the plane perpendicular to the rotation axis and the observational line-of-sight to $\theta = 35.78^{+2.13}_{-1.88}$ degrees.

In the multiphase model the best constrained parameters by the observational data are the clump velocity dispersion ~~$\sigma_{\rm cl} = 69^{+17}_{-15}$ km s^{-1}, the clumps outflowing velocity $v_{\infty,{\rm cl}} = 79^{+73}_{-42}$ km s^{-1}~~ $\sigma_{\rm cl}$ =54.3 $\pm$ 0.6 km s^{-1}, the clump's outflowing velocity $v_{\infty,{\rm cl}}$ =54.3 $\pm$ 5.1 km s^{-1} and the fraction of the Lyα emission that is coming from the cold clumps ~~$P_{cl} = 0.78^{+0.16}_{-0.43}$. The multiphase model assumes that the clouds are distributed over a sphere of 5kpc in radius, close to the $\approx$ 4kpc physical size of Tololo 1214-277as determined by optical imaging. The assumed physical size and the velocity dispersion $\sigma_{\rm cl}$ correspond to~~ $P_{\rm cl}$ =0.96 $\pm$ 0.01.

Assuming that the clumps are located in a spherical region of radius $r_s = 2.25$ kpc (corresponding to Tololo 1214-277's estimated 3D half-light radius), this corresponds to dynamical masses of $M_{\rm dyn} = 3.2^{+1.6}_{-1.0} \times 10^{10} M_\odot$ and $M_{\rm dyn} = 2.31 \pm 0.04 \times 10^9$ $M_\odot$ for the rotation and multiphase models, respectively.

Tololo 1214-277's stellar mass is $M_\star = 1.45 \pm 0.45 \times 10^8 M_\odot$ [10] and its total neutral HI mass is $M_{\rm HI} < 2.65 \times 10^8$ M$_\odot$ [11] ; the dynamical mass is at least 6 to 80 times the baryonic mass, depending if one considers the multiphase or rotation estimate.

We lean towards the lower dynamical mass estimate from the multiphase model as it seems easier to reconcile with the following two astrophysical mechanisms for its origin. The first way to explain a dynamical mass of ~~$M_{\rm dyn} = 2.8^{+1.3}_{-1.2} \times 10^9$ $M_\odot$. In the rotation model assuming reasonable bounds for the number density of neutral Hydrogen atoms ($0.01 < n/{\rm atoms\ cm}^{-3} < 0.1$) and using $\tau = 10^7$ the radius of the emission region can be bracketed to be in $0.55 < r_s/{\rm kpc} < 5.5$. Using $V_{\rm max} = 300$km s^{-1}, we find a dynamical mass range of $5.45 \times 10^9 M_\odot < M_{\rm dyn} < 5.45 \times 10^{10} M_\odot$~~ $10^9 M_\odot$ in a sphere of 2 kpc could be having a dark matter halo of at least 10^{12} M$_\odot$ in mass [12], which leaves open the question as to why Tololo 1214-277 is not more similar to the Milky Way galaxy as it is hosted by a dark matter halo of similar mass. A second possibility is that Tololo 1214-277 hosts a supermassive black hole of $10^9 M_\odot$. This is almost two orders of magnitude higher than the supermassive black hole found in the compact dwarf galaxy M60-UCD1 [13], which has a similar stellar mass as Tololo 1214-277. This would leave open the question about the formation process of such a system.

~~Which solution is more plausible? If~~ Another perspective to appreciate the atypically high dynamical mass estimates comes from the observed scaling relations for dwarf galaxies. Assuming that Tololo 1214-277 followed the fundamental plane relationship between its mean surface brightness I_e, the projected half-light radius R_e and the velocity dispersion σ, described by $\log I_e = 1.6 \log \sigma - 1.21 \log R_e + 0.55$ ~~[12, 14]~~ [14], the expected velocity dispersion ~~would~~ should be on the order of ~~47 ± 3~~ 5 ± 1 km s^{-1}, which ~~only presents a small tension with the multiphase model. The solution of a high rotational velocity pushes Tololo 1214-277~~is a factor of $\sim$ 10 - 60 lower than the results from the multiphase and rotation models, respectively. These are equivalent to factors of $\sim$ 100 - 3600 on the dynamical mass. Once again, Tololo 1214-277 ~~outside the scaling relationship for dwarfs. One could account for the high velocities if the galaxy had a supermassive black hole accounting for the mass that cannot be explained by baryonic or dark mass. The economy of assumptions makes it more reasonable to expect that the multiphase model could be a better match to reality~~seems to be significantly more massive than expected.

A ~~future observational test~~ new observational test is needed to clarify the physical nature of Tololo 1214-277~~would require~~. We suggest that integral field unit measurements spatially resolving its spatial extent are up to the task. Tololo 1214-277 spans a region of 4 arcseconds, an instrument such as the Multi Unit Spectroscopic Explorer [15] with its nominal 0.2 arcseconds spatial sampling over a 1.0 arcminute field in wide-field mode could provide a coarse mapping of different ionization lines to infer a kinematic map. Another observational test includes the measurement of the ~~escape fraction of Ly continuum ionizing radiation~~Lyα ionizing continuum escape fraction. In the rotational model this fraction should be zero, while the multiphase model predicts that ~~in this case~~ averaging over all sightlines it should be around $0.5^{+1.0}_{-0.4}$%, with the possibility of strong variations depending on viewing angle.

All in all, the mere existence of a strong LAE galaxy with a broad, symmetric line is interesting. It raises the question whether some high redshift LAEs have asymmetric lines because the blue half was truncated by the intergalactic medium. In this case the Lyα radiation could emerge as a low surface brightness glow, which may be connected to Lyα halos, while also influencing the way LAEs can be used as a probe of reionization [16].

These findings demonstrate the importance of including rotation and multiphase conditions as ~~a feature~~ features to model the Lyα line in high redshift galaxies. ~~If the estimated velocity dispersion~~ Additionally, if the hypothesis of a

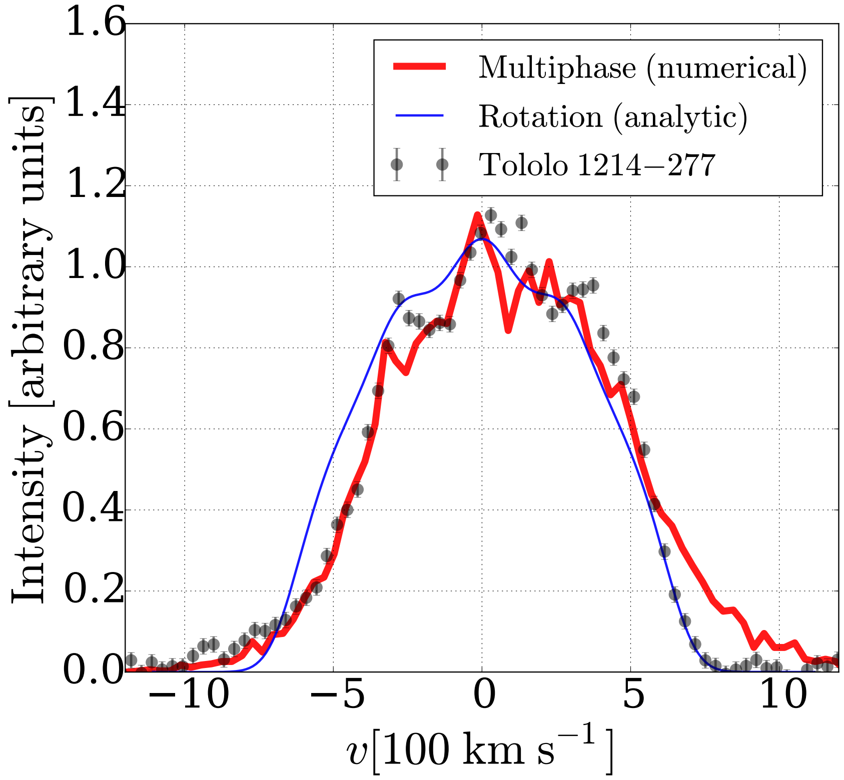

Figure 1: **Broad, single peaked and symmetric Ly-α emission of Tololo 1214-277.** Dots correspond to the observational data. The line shows the results of our best model from a full radiative transfer simulation both for the rotation and multiphase models.

supermassive black hole in Tololo 1214-277 proves to be consistent with future observational kinematic maps, it could ~~provide a new way to study velocity dispersions in distant gas rich starbursting galaxies, opening the possibility to study the dynamical~~ correspond to a so far undetected supermassive black hole in a dwarf galaxy, providing a new way to test and probe theories on the co-evolution of galaxies and ~~dark matter halos~~ black holes in the first generation of galaxies.

References

[1] R. B. Partridge and P. J. E. Peebles, "Are Young Galaxies Visible?," *ApJ*, vol. 147, p. 868, Mar. 1967.

[2] A. Dey, H. Spinrad, D. Stern, J. R. Graham, and F. H. Chaffee, "A Galaxy at z = 5.34," *ApJL*, vol. 498, pp. L93–L97, May 1998.

[3] G. Östlin, M. Hayes, F. Duval, A. Sandberg, T. Rivera-Thorsen, T. Marquart, I. Orlitová, A. Adamo, J. Melinder, L. Guaita, H. Atek, J. M. Cannon, P. Gruyters, E. C. Herenz, D. Kunth, P. Laursen, J. M. Mas-Hesse,

G. Micheva, H. Otí-Floranes, S. A. Pardy, M. M. Roth, D. Schaerer, and A. Verhamme, "The Lyα Reference Sample. I. Survey Outline and First Results for Markarian 259," *ApJ*, vol. 797, p. 11, Dec. 2014.

[4] T. E. Rivera-Thorsen, M. Hayes, G. Östlin, F. Duval, I. Orlitová, A. Verhamme, J. M. Mas-Hesse, D. Schaerer, J. M. Cannon, H. Otí-Floranes, A. Sandberg, L. Guaita, A. Adamo, H. Atek, E. C. Herenz, D. Kunth, P. Laursen, and J. Melinder, "The Lyman Alpha Reference Sample. V. The Impact of Neutral ISM Kinematics and Geometry on Lyα Escape," *ApJ*, vol. 805, p. 14, May 2015.

[5] T. X. Thuan and Y. I. Izotov, "Nearby Young Dwarf Galaxies: Primordial Gas and Lyα Emission," *ApJ*, vol. 489, pp. 623–635, Nov. 1997.

[6] A. Verhamme, D. Schaerer, and A. Maselli, "3D Lyα radiation transfer. I. Understanding Lyα line profile morphologies," *A&A*, vol. 460, pp. 397–413, Dec. 2006.

[7] M. Gronke, P. Bull, and M. Dijkstra, "A Systematic Study of Lyman-α Transfer through Outflowing Shells: Model Parameter Estimation," *ApJ*, vol. 812, p. 123, Oct. 2015.

[8] J. N. Garavito-Camargo, J. E. Forero-Romero, and M. Dijkstra, "The Impact of Gas Bulk Rotation on the Lyα Line," *ApJ*, vol. 795, p. 120, Nov. 2014.

[9] M. Gronke and M. Dijkstra, "Lyα Spectra from Multiphase Outflows, and their Connection to Shell Models," *ApJ, accepted*, Apr. 2016.

[10] S. C. Madden, A. Rémy-Ruyer, M. Galametz, D. Cormier, V. Lebouteiller, F. Galliano, S. Hony, G. J. Bendo, M. W. L. Smith, M. Pohlen, H. Roussel, M. Sauvage, R. Wu, E. Sturm, A. Poglitsch, A. Contursi, V. Doublier, M. Baes, M. J. Barlow, A. Boselli, M. Boquien, L. R. Carlson, L. Ciesla, A. Cooray, L. Cortese, I. De Looze, J. A. Irwin, K. Isaak, J. Kamenetzky, O. Ł. Karczewski, N. Lu, J. A. MacHattie, B. O'Halloran, T. J. Parkin, N. Rangwala, M. R. P. Schirm, B. Schulz, L. Spinoglio, M. Vaccari, C. D. Wilson, and H. Wozniak, "An Overview of the Dwarf Galaxy Survey (PASP, 125, 600, [2013]) - Corrigendum," *PASP*, vol. 126, pp. 1079–1080, Nov. 2014.

[11] S. A. Pustilnik and J.-M. Martin, "H I study of extremely metal-deficient dwarf galaxies. I. The Nançay radio telescope observations of twenty-two objects," *A&A*, vol. 464, pp. 859–869, Mar. 2007.

[12] E. J. Tollerud, J. S. Bullock, G. J. Graves, and J. Wolf, "From Galaxy Clusters to Ultra-faint Dwarf Spheroidals: A Fundamental Curve Connecting Dispersion-supported Galaxies to Their Dark Matter Halos," *ApJ*, vol. 726, p. 108, Jan. 2011.

[13] A. C. Seth, R. van den Bosch, S. Mieske, H. Baumgardt, M. D. Brok, J. Strader, N. Neumayer, I. Chilingarian, M. Hilker, R. McDermid, L. Spitler, J. Brodie, M. J. Frank, and J. L. Walsh, “A supermassive black hole in an ultra-compact dwarf galaxy,” *Nature*, vol. 513, pp. 398–400, Sept. 2014.

[14] G. J. Graves, S. M. Faber, and R. P. Schiavon, “Dissecting the Red Sequence. II. Star Formation Histories of Early-Type Galaxies Throughout the Fundamental Plane,” *ApJ*, vol. 698, pp. 1590–1608, June 2009.

[15] R. Bacon, J. Vernet, E. Borisova, N. Bouché, J. Brinchmann, M. Carollo, D. Carton, J. Caruana, S. Cerda, T. Contini, M. Franx, M. Girard, A. Guerou, N. Haddad, G. Hau, C. Herenz, J. C. Herrera, B. Husemann, T.-O. Husser, A. Jarno, S. Kamann, D. Krajnovic, S. Lilly, V. Mainieri, T. Martinsson, R. Palsa, V. Patricio, A. Pécontal, R. Pello, L. Piqueras, J. Richard, C. Sandin, I. Schroetter, F. Selman, M. Shirazi, A. Smette, K. Soto, O. Streicher, T. Urrutia, P. Weilbacher, L. Wisotzki, and G. Zins, “MUSE Commissioning,” *The Messenger*, vol. 157, pp. 13–16, Sept. 2014.

[16] M. Dijkstra, “Lyα Emitting Galaxies as a Probe of Reionisation,” *PASA*, vol. 31, p. e040, Oct. 2014.

[17] Y. I. Izotov, P. Papaderos, N. G. Guseva, K. J. Fricke, and T. X. Thuan, “Deep VLT spectroscopy of the blue compact dwarf galaxies Tol 1214-277 and Tol 65,” *A&A*, vol. 421, pp. 539–554, July 2004.

[18] D. G. Hummer and P. J. Storey, “Recombination-line intensities for hydrogenic ions. I - Case B calculations for H I and He II,” *MNRAS*, vol. 224, pp. 801–820, Feb. 1987.

[19] C. W. Engelbracht, G. H. Rieke, K. D. Gordon, J.-D. T. Smith, M. W. Werner, J. Moustakas, C. N. A. Willmer, and L. Vanzi, “Metallicity Effects on Dust Properties in Starbursting Galaxies,” *ApJ*, vol. 678, pp. 804–827, May 2008.

[20] M. Eskew, D. Zaritsky, and S. Meidt, “Converting from 3.6 and 4.5 μm Fluxes to Stellar Mass,” *AJ*, vol. 143, p. 139, June 2012.

[21] K. G. Noeske, P. Papaderos, L. M. Cairós, and K. J. Fricke, “New insights to the photometric structure of Blue Compact Dwarf galaxies from deep Near-Infrared studies. I. Observations, surface photometry and decomposition of surface brightness profiles,” *A&A*, vol. 410, pp. 481–509, Nov. 2003.

[22] J. E. Forero-Romero, G. Yepes, S. Gottlöber, S. R. Knollmann, A. J. Cuesta, and F. Prada, “CLARA’s view on the escape fraction of Lyman α photons in high-redshift galaxies,” *MNRAS*, vol. 415, pp. 3666–3680, Aug. 2011.

[23] D. Foreman-Mackey, D. W. Hogg, D. Lang, and J. Goodman, “emcee: The MCMC Hammer,” *PASP*, vol. 125, pp. 306–312, Mar. 2013.

[24] P. Laursen, F. Duval, and G. Östlin, “On the (Non-)Enhancement of the Lyα Equivalent Width by a Multiphase Interstellar Medium,” *ApJ*, vol. 766, p. 124, Apr. 2013.

$\alpha(2000)^a$	12h17min17.1s
$\delta(2000)^b$	-28d02m32s
l, b (deg)	294, 34
m_V	17.5
M_V	-17.6
v(km s^{-1})	7795
Ly-α (erg cm^{-2} s^{-1} Å^{-1})	8.1×10^{-14}
Ly-α EW	70Å
Hβ (erg cm^{-2} s^{-1} Å^{-1})	1.62×10^{-14}
21cm (Jy km s^{-1})	< 0.10

Table 1: Basic observational characteristics of TOL1214-277 [5]

Tololo 1214-277 characteristics

~~Tololo 1214-277~~Tololo 1214-277 receding velocity is 7785 ± 50km s^{-1}, which translates into a distance of 106.6 Mpc (~~Hubble constant~~ with the Hubble constant H_0=73 Mpc km ~~$^{-1}$ s^{1}~~s^{-1}) Its metallicity is $\sim Z_{\odot}/24$ [17] as derived from optical spectroscopy.

The observed flux for the Lyman alpha line is $\sim 8.1 \times 10^{-14}$ erg cm^{-2} s^{-1} [5] and a Equivalent Width of 70Åand its Hβ flux is 1.62×10^{-14} erg cm^{-2} s^{-1} Å-1 [17] which gives a Lyα/Hβ flux ratio of 4.9±0.1. The Ly-α flux values correspond to luminosities of $L_{Ly\alpha} = 2.2 \times 10^{42}$ erg s^{-1} over a 20Åbandwidth, which in turns translates into a star formation rate of 2.0 M$_{\odot}$ yr^{-1} using a standard conversion factor between luminosity and star formation rate of 9.1×10^{-43} $L_{Ly\alpha}$ M$_{\odot}$ yr^{-1}. The absolute magnitude in the V band translates into a luminosity of 8.9×10^8 L$_{\odot}$. Comparing this ratio with the theoretical expectation from case B recombination of 23.3 [18] one can estimate an escape fraction of 20% for Lyα radiation. The bolometric UV luminosity is $9.43 \pm 1.94 \times 10^8$ L$_{\odot}$ as measured by GALEX.

~~The optical emission comes from a region with approximate diameter 4 kpc [?] .~~

There is an upper limit for the integrated flux of < 0.10 Jy km s^{-1}, which translates into a upper limit for the HI mass of $M < 2.65 \times 10^8$ M$_{\odot}$ [11].

The near-infrared fluxes at 3.6 μm and 4.5 μm are $7.71 \pm 0.55 \times 10^{-5}$ Jy and $7.98 \pm 0.71 \times 10^{-5}$ Jy [19]. Using a ~~convertion betwen~~ conversion between fluxes and stellar mass ~~calibrted~~ calibrated on the Large Magellanic Cloud $M_{\star} = 10^{5.65} \times F_{3.6}^{2.85} \times F_{4.5}^{-1.85} \times (D/0.05)^2 M_{\odot}$, where fluxes are in Jy and D is the luminosity distance to the source in Mpc, we find $M_{\star} = 1.45 \pm 0.45 \times 10^8 M_{\odot}$, with a 30% uncertainty coming from the ~~callibration~~ calibration process [20].

We computed the projected half-luminosity radius to be $R_s = 1.5 \pm 0.1$ kpc from the surface intensity profiles reported by. [21] . Assuming spherical geometry, one can translate this value into a 3D half-luminosity radius of $r_s = 3R_s/2 = 2.25$ kpc.

The Rotation Model

The rotation model corresponds to the work presented in [8] based on the Monte Carlo code `CLARA` [22] . In that model the Ly-α photons are propagated within a spherical and homogeneous cloud of HI gas undergoing solid body rotation. The sphere is fully characterized by three parameters: the HI optical depth τ measured from the center to its surface, the HI temperature T, and the linear surface velocity $V_{\rm max}$. Photons are emitted at their natural frequency from the center of the sphere. Including the effect of dust only changes the overall line normalization but not its shape. The results we report in the main body of the paper do not include any dust model. In ~~the current work, the radiative transfer simulations were done using Monte Carlo simulations with the code CLARA [22]~~ this letter we use an analytical solution that captures the most important effects of rotation onto the Lyα line.

The first important effect of rotation is that it breaks the spherical symmetry of the static case. Now the line's observed morphology depends on the angle θ between the line-of-sight (LOS) and the rotation axis. LOS parallel to the rotation axis tend to observed the line without any modification from rotation, while the perpendicular LOS will observe a maximal change in the line's morphology due to rotation.

The main change in the line's morphology is that it broadens and the intensity at the center increases. For high enough rotational velocities the intensity at the peak's center increases so much that the line goes from double to single peaked, sometimes slightly triple peaked. This is the feature that allows this model to fit the observational features of Tololo 1214-277.

~~There is~~ [8] derive a concise analytical description for those features. This description takes into account how different parts of the sphere's surface shift in frequency the Lyα photons. Different shifts in frequency come from different values for the projected velocity along the LOS. ~~As presented in [22] , using~~ Using the analytical solution for the Lyα~~sphectra~~ spectra of a static sphere plus the right frequency shifts computed from geometrical considerations, one is able to ~~produce~~ compute an analytical solution for the rotating sphere that reproduces the main features found using the full numerical simulation.

The analytical solution for the rotation sphere was the base to perform the Markov Chain Monte Carlo ~~Calculation~~ (MCMC) calculation using the `emcee` ~~implementation. We~~ Python library [23] . `emcee` is an open source optimized implementation of the affine-invariant ensemble sampler for MCMC. The algorithm creates a number of walkers that, during a sufficient number of steps, generate parameters' combinations for a specific model. For each time, the code calculates the likelihood of the combination with respect to the observational data. The walkers ecplore the parameter space sampling the likelihood function.

MCMC methods are optimal for sampling parameters at a high number of dimensions. In this case we explore flat priors on ~~$V_{\rm max}$ $\log_{10}\tau$, $\log_{10}T$ and θ using XX steps~~ four parameters: $200 < V_{\rm max}/{\rm km\ s^{-1}} < 600$, $6.0 < \log_{10}\tau < 9.0$, $4.0 < \log_{10} T/10^4{\rm K} < 4.5$ and $0 < \theta < 90$ using 500 steps with 24 walkers for a

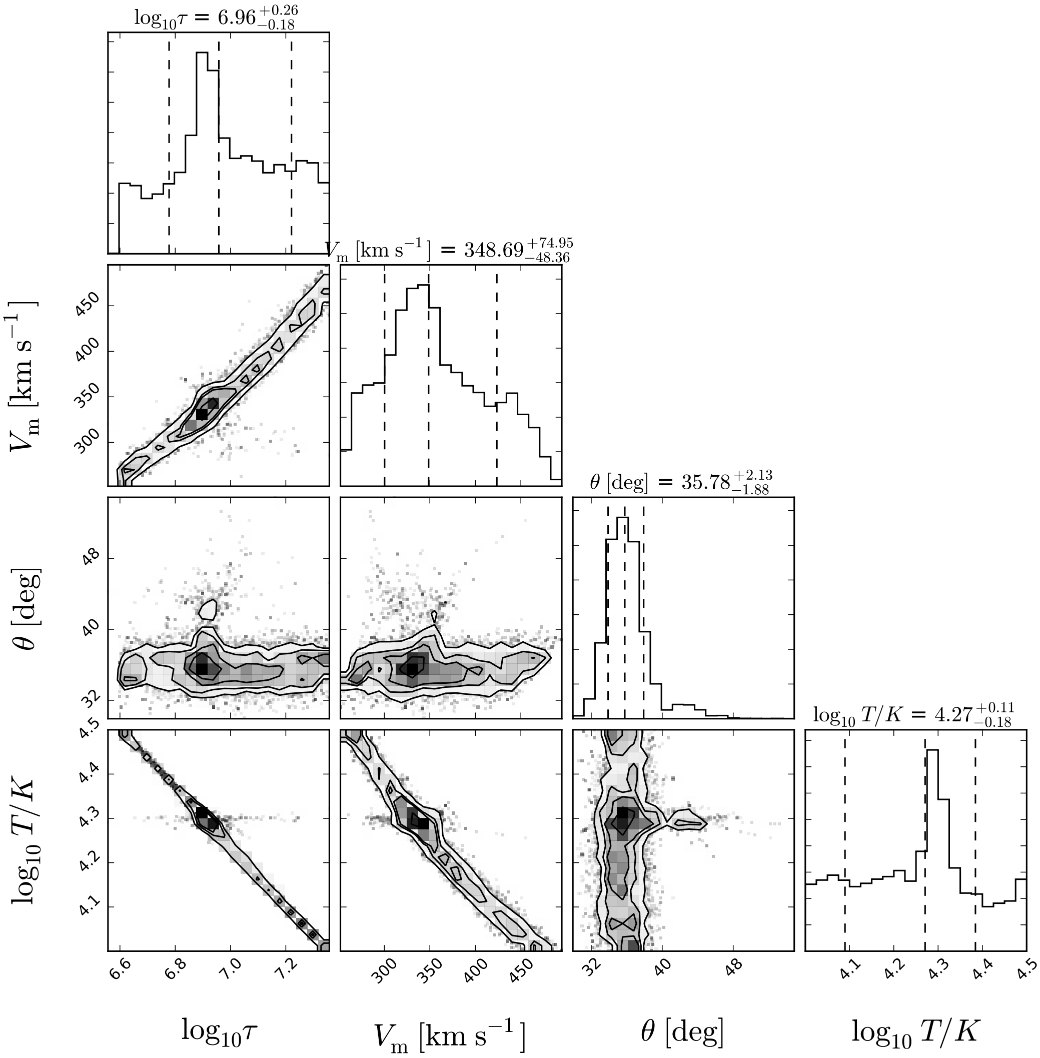

Figure 2: **Results from the Markov Chain Monte Carlo ~~compuation~~ computation for the rotation model.** The dotted vertical lines in the outer histograms represent the percentiles 16%, 50% and 84%.

total of 12000 points in the chain. The results are summarized in Figure ~~XX~~2. From this model we find that the fiducial parameters that could explain the broad features in Tololo 1214-277 are $V_{\rm max} = 348^{+75}_{-48}$ km s^{-1}, $\log\tau = 6.96^{+0.26}_{-0.18}$, $\log_{10} T/\mathrm{K} = 4.27^{+0.11}_{-0.18}$ and $\theta = 35.78^{+2.13}_{-1.88}$ degrees.

The Multiphase Model

The idealized multiphase model consists of spherical, cold, dens clumps of neutral hydrogen (and dust) embedded in a hot, ionized medium. The clumps also have a random and an outflowing velocity component which totals the number of parameters describing the model to be 14.

In order to map out this large parameter space, we randomly drew 2500 sets of parameters within a observationally realistic range (based on the considerations of [24]) yielding a large variety of single-, double- and triple-peaked spectra. The full analysis of the the spectral features as well as more details on the radiative transfer are presented in [9].

For the current work, we computed the χ^2 for each of the 2500 ~~parameters yielding the best fit parameters of (...). Here, the subscripts $_{\rm cl}$ and $_{\rm ICM}$ stand for the quantities filling the clumps and the medium between the clumps, respectively. Furthermore,~~ models. We selected the best 50 models with the lowest χ^2. The χ^2 gap in those 50 models is close to 3000, the lowest χ^2 is close to 1200. The total number of degrees of freedom is 104.

Then we performed a Kolmogorov-Smirnov test to compare each parameter distribution in the best 50 models against the parent distribution of 2500 models. If we obtain a p-value < 0.05 for a given parameter, we conclude that this parameter does influence the χ^2 fit, as the distribution for the best χ^2 models is statistically different to the distribution from the global sample of 2500 models.

From this test we found that ~~some parameters such as the magnitude of the random clump motion~~ only three parameters influence the χ^2: the clump outflow velocity $v_{\infty,\rm cl}$ (p-value 10^{-18}), the clump velocity dispersion $\sigma_{\rm cl}$ ~~improved the fit significantly whereas others did not~~(p-value 10^{-4}) and the probability that the Lyα emission comes from the clumps $P_{\rm cl}$ (p-value 10^{-4}).

The best values for those parameters that we report here correspond to the values that produce the minimum χ^2. The 1-σ uncertainty comes from a parabolic fit to the χ^2 as a function of $v_{\infty,\rm cl}$, $\sigma_{\rm cl}$, $P_{\rm cl}$ around its corresponding minimum. Under these conditions we find $\sigma_{\rm cl}$ =54.3 ± 0.6 km s^{-1}, $v_{\infty,\rm cl}$ =54.3 ± 5.1 km s^{-1} and $P_{\rm cl}$ =0.96 ± 0.01.

Qualitatively as Tololo 1214-277 possesses a very wide spectrum which can be achieved by subsequent scatterings off (relatively) fast moving clumps while the multi-phase nature (i.e., the existence of low-density channels) ensures the high flux at line center as observed.

~~Physical Interpretation~~Dynamical Mass Estimates

~~Both the rotation and~~ Having constrains for velocity dipersion σ of some dynamical tracers (clumps in the case of the multiphase model~~constrain the typical velocity v of the HI gas, with and additional constrain on the typical size for the emission region~~) in a spherical system located in a region of size r we estimate the dynamical mass within r~~on could estimate a dynamical mass with~~

$$M_{\rm dyn} = \frac{v^2 r}{G} = 1.16\times 10^9 \left(\frac{v}{100\ {\rm km\ s^{-1}}}\right)^2 \left(\frac{r}{\rm kpc}\right) M_{\odot}$$

~~From the multiphase model we obtained $v = 69^{+17}_{-15}$ km s^{-1}and $r = 5$ kpc. This corresponds to a dynamical mass of $M_{\rm dyn} = 2.8^{+1.3}_{-1.2}\times 10^9\ M_{\odot}$ which is at least 5 times the HI mass plus the stellar mass estimated from observations~~.

~~In the rotation model the size of the spherical region, r_s, can be infered from the relationship $\tau = \sigma_0 n r_s$, where $\sigma_0 = 5.898 \times 10^{-14}\mathrm{cm}^{-2}$ is the Lymanα cross section at the line's center, n is the number density. This expresion can be rewritten as~~

$$r_s = 0.055 \left(\frac{\tau}{10^7}\right) \left(\frac{\text{atoms cm}^{-3}}{n}\right) \text{kpc.}$$

~~Using this result and assuming a bound for the number density of $0.01 < n/\text{atoms cm}^{-3} < 0.1$ we have $0.55 < r_s/\text{kpc} < 5.5$.~~

$$M_{\rm dyn} = 3\frac{\sigma^2 r}{G} = 3.48 \times 10^9 \left(\frac{\sigma}{100 \text{ km s}^{-1}}\right)^2 \left(\frac{r}{\text{kpc}}\right) M_{\odot} \tag{1}$$

~~This is consistent with the constraint on the total HI mass and the optical depth τ_0 as we show next. The total HI mass can be approximated as $M_H = \frac{4\pi}{3} m_H n r_s^3$, where $m_H = 1.67 \times 10^{-24}$ gr is the mass of a single Hydrogen atom. This allows us to write the total hydrogen mass as~~

$$M_H = 5.70 \times 10^6 \left(\frac{\tau}{10^7}\right) \left(\frac{r_s}{\text{kpc}}\right)^2 M_{\odot}$$

~~The uppper limit from the HI mass non-detection imposes $r_s < 6.81$ kpc, which is consistent with the bound we found in the first place, as we wanted to show.~~ As described in the main the letter, we use the 3D half-luminosity radius, r_s, as the typical size for the HI region.

~~Using those size bounds for the spherical model we find a constrain for~~ In the case of rotational velocity v in a region of size r we estimate the dynamical mass ~~of $5.45 \times 10^9 M_{\odot} < M_{\rm dyn} < 5.45 \times 10^{10} M_{\odot}$.~~ by

$$M_{\rm dyn} = \frac{v^2 r}{G} = 1.16 \times 10^9 \left(\frac{v}{100 \text{ km s}^{-1}}\right)^2 \left(\frac{r}{\text{kpc}}\right) M_{\odot} \tag{2}$$